Received: 15 July 2020 | Revised: 14 July 2021 | Accepted: 21 October 2021

DOI: 10.1002/JLB.5AB0720-446RR

JLB JOURNAL OF LEUKOCYTE BIOLOGY

BRIEF CONCLUSIVE REPORT

CCR7$^+$ dendritic cells sorted by binding of CCL19 show enhanced Ag-presenting capacity and antitumor potency

Paul Burgoyne[1,2] | Alan J Hayes[1,2] | Rachel S Cooper[2] | Michelle L Le Brocq[1] | Christopher AH Hansell[1] | John DM Campbell[1,2] | Gerard J Graham[1]

[1] Chemokine Research Group, Institute of Infection, Immunity and Inflammation, University of Glasgow, Glasgow, UK

[2] Scottish National Blood Transfusion Service, Jack Copland Centre, Edinburgh, UK

Correspondence
Prof. John DM Campbell (lead), SNBTS, 52 Research Avenue North, Edinburgh EH17 7QT, Edinburgh, UK.
Email: john.campbell4@nhs.scot
Prof. Gerard J Graham, Chemokine Research Group, Institute of Infection, Immunity and Inflammation, University of Glasgow, 120 University Place, Glasgow, G12 8TA, UK.
Email: gerard.graham@glasgow.ac.uk

Abstract

Dendritic cell therapy has been a promising addition to the current armory of therapeutic options in cancer for more than 20 years but has not yet achieved breakthrough success. To successfully initiate immunity, dendritic cells have to enter the lymph nodes. However, experience to date of therapeutic dendritic cell administration indicates that this is frequently an extremely inefficient process. The major regulator of dendritic cell migration to the lymph nodes is the chemokine receptor CCR7 and in vitro generated dendritic cells typically display heterogeneous expression of this receptor. Here we demonstrate that positive selection for the dendritic cell subpopulation expressing CCR7, using a chemically-synthesized ligand:CCL19, enriches for cells with enhanced lymph node migration and Ag presentation competence as well as a chemokine expression profile indicative of improved interactions with T cells. This enhanced lymph node homing capacity of enriched CCR7+ cells is seen in comparison to a population of unsorted dendritic cells containing an equivalent number of CCR7+ dendritic cells. Importantly, this indicates that separating the CCR7+ dendritic cells from the CCR7− cells, rather than simple CCL19 exposure, is required to affect the enhanced lymph node migration of the CCR7+ cells. In models of both subcutaneous and metastatic melanoma, we demonstrate that the dendritic cells sorted for CCR7 expression trigger enhanced CD8 T-cell driven antitumor immune responses which correlate with reduced tumor burden and increased survival. Finally, we demonstrate that this approach is directly translatable to human dendritic cell therapy using the same reagents coupled with clinical-grade flow-cytometric sorting.

KEYWORDS
cancer, chemokines, translation, vaccines, cellular therapy

1 | INTRODUCTION

Cellular therapy is an increasingly important treatment option in a range of clinical contexts including cancers and inflammatory/immune disorders.[1–3] However, success is often limited by the mixed ability of the cells to home to, or be retained in, appropriate in vivo "therapeutic" sites. In the context of dendritic cell (DC) therapy the limited competence of therapeutically administered DCs to home to lymph nodes (LNs) from the injection site[4–6] has contributed to a marked inefficiency of this therapeutic approach. Despite attempts to improve this,

insufficient LN homing remains a frequent impairment to effective DC therapy. New approaches are therefore urgently needed to optimize such cell therapies.

Chemokines are central to in vivo tissue-homing of cells[7] and humans have approximately 45 chemokines many of which are expressed at select in vivo sites, or in specific inflamed contexts. Chemokines are broadly characterized as being inflammatory or homeostatic according to the in vivo contexts in which they function. The selective nature of chemokine expression ensures the attraction of cells bearing appropriate cognate chemokine receptors[8] to specific tissues. One of the classic paradigms for chemokine receptor involvement in cellular homing focuses on CCR7,[9] which is essential for cellular homing to, and positioning within, LNs.[10] During DC maturation, up-regulation of CCR7[9] ensures efficient LN migration to facilitate communication with T cells. Overexpression of CCR7 in DCs in murine models has been clearly linked with increased LN homing[11,12] and in human cancer patients, the extent of CCR7 expression on DCs correlates with the magnitude of the tumor-infiltrating lymphocyte population.[13] However, to date, attempts to increase LN homing competence of cells, either by manipulating CCR7 expression or by other means, have frequently been cumbersome and of limited applicability to the clinical context.[11,12,14–16]

We have developed a novel approach to help address this issue.[17] While DC populations generated in vitro for therapeutic purposes invariably express heterogeneous levels of CCR7, we have shown that selection of the subpopulation expressing CCR7 leads to a 'fitter' cellular product with enhanced LN homing. Typically such cell-selection would be carried out using Abs but high-quality Abs are not available for the majority of chemokine receptors. We therefore use chemokines labeled with biotin and/or fluorophores, rather than Abs, to select for cognate receptor-expressing cells.[17,18] Specifically for sorting CCR7-expressing cells we use streptavidin-tetramerized biotinylated CCL19 (bCCL19).

Here, we have used models of primary and metastatic cancer to show enhanced immune priming by CCR7-sorted DCs with improved outcomes in the tumor models. This study demonstrates the value of preselection of DCs for LN homing potential and highlights a potentially important novel development for therapeutic approaches to DC use in cancer vaccinology.

2 | BRIEF MATERIALS AND METHODS

2.1 | Animals

C57BL/6 mice were from Charles River Laboratories, and OT-I mice were bred and maintained in house. All experiments were approved by the University of Glasgow Ethical Review Committee and performed under the auspices of a UK Home Office Licence.

2.2 | Isolation of mouse and human cells

Bone marrow-derived DCs (BMDCs) were generated as outlined in Supplementary Materials And Methods and as described previously.[17] Murine T cells were isolated from harvested peripheral LNs of 8 week-old OT-I mice, by homogenizing LNs through a cell strainer, and plated at 2×10^6 cells/ml in mRPMI until use. Human buffy coats were obtained from SNBTS under appropriate sample governance and CD14+ monocyte-derived DCs (moDCs) generated as described previously[17,26] and T cell populations cultured in vitro as described in Supplementary Materials And Methods. BMDCs and moDCs were sorted for CCR7 expression by labeling with biotinylated chemically synthesized CCL19 (bCCL19, Almac Sciences, UK)[17] as outlined in Supplementary Materials And Methods, "Mock sorted" DCs were processed in labeling buffer only, followed by cell sorting of the entire population based on the same scatter gates as the bCCL19-labeled cells. For some in vivo experiments, cells were labeled with the bCCL19 reagent but not sorted into CCR7 enriched or depleted fractions.

2.3 | In vitro T cell stimulation

To assess DC stimulation of T cell responses, T cells were co-cultured in vitro with either CCR7-sorted or unsorted DCs, or 20 U/ml IL-2 alone, at a ratio of 1:25 DCs:T cells in complete RPMI. Cultures were maintained for 7 days (mouse) or 10 days (human), with media replaced as necessary.

2.4 | Animal experiments: Footpad migration

BMDC cultures were mock sorted, or sorted into a CCR7+population. Both populations were labeled using PKH67 dye (Sigma-Aldrich) as per the manufacturer's guidelines. Cells were injected into the contralateral footpads of mice and after 48 h the draining popliteal LNs and footpads were collected for enumeration of DCs in each tissue. A total of 10^6 $CCR7^+$ sorted cells were injected. The mock-sorted cells were formulated to contain a total of 10^6 $CCR7^+$ cells to normalize the numbers of $CCR7^+$ cells administered (typically a total of 1.5×10^6 cells). To analyze cells present in the footpad at 48 h, the tissue was digested using 2 mg/ml Collagenase IV, 2 mg/ml hyaluronidase, and 0.1 mg/ml DNase I (all Invitrogen) in RPMI for 20 min at 37°C.[19]

2.5 | Animal experiments: Tumor models

To generate subcutaneous tumors, 8-week old male mice were injected on the right flank with 5×10^5 B16.ova cells.[24] Tumors were allowed to grow until any animal in the cohort carried a tumor of 12 mm in diameter (commonly first reached in control groups), triggering a cull of all subjects. The number of days to reach this point is detailed in each experimental section. To generate metastatic tumors, 8-week old male mice were injected intravenously with 5×10^5 B16.ova cells and culled after a set period of 14 days.[24] All tumor experiments had at least 5 animals per group.

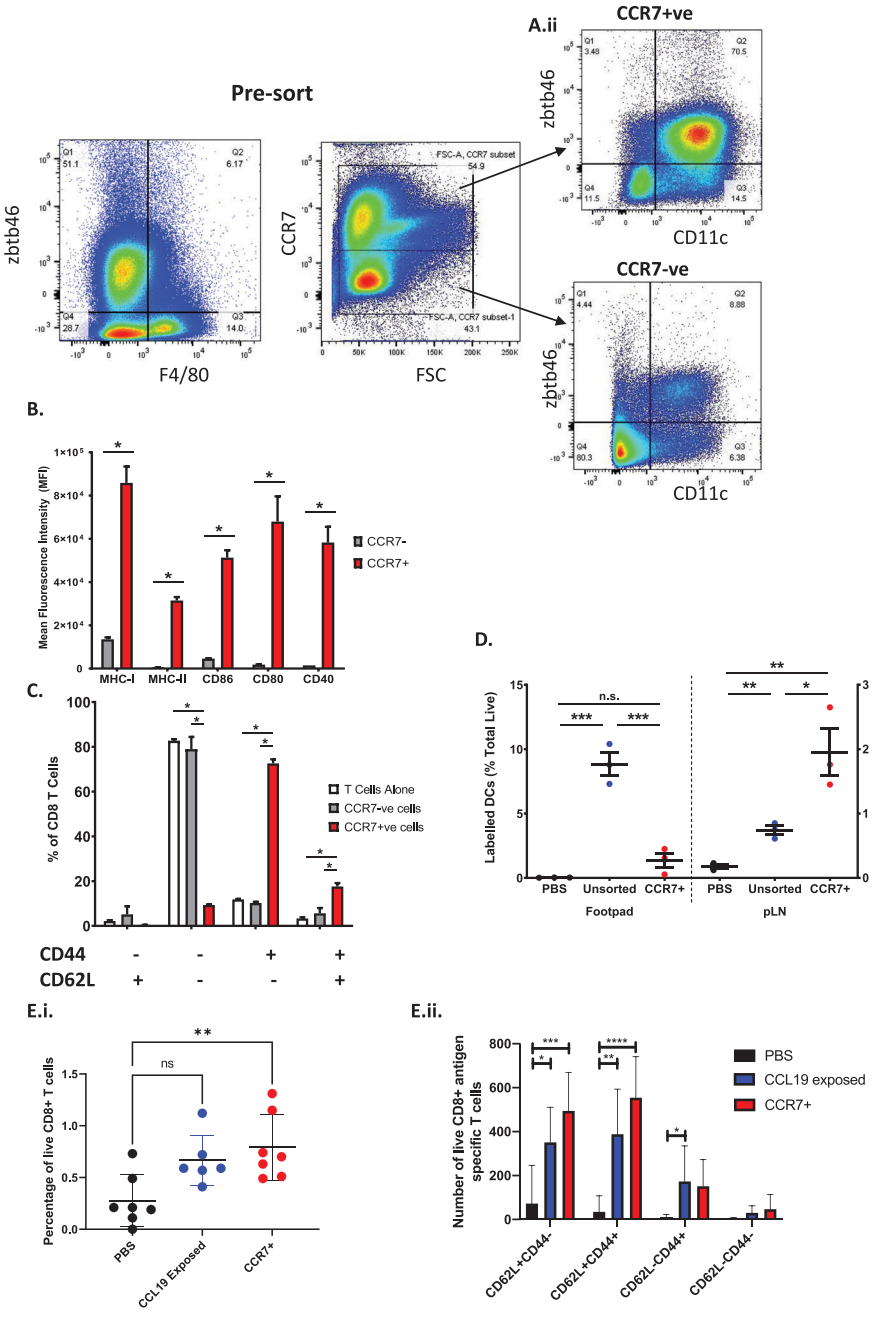

FIGURE 1 CCR7-sorted dendritic cells are enhanced for Ag presentation. (A) (i) BMDC cultures are heterogeneous for CCR7 expression (FSC = Forward Scatter) post-incubation with Ag, LPS, and TNF-α. (ii) CCR7$^+$ cells are a majority CD11c+ zbtb46+ population of DCs, CCR7$^-$ cells are a mixed population containing a minority CD11c and zbtb46$^+$ cells. (B) Expression of markers of Ag-presenting competence and T cell co-stimulation in CCR7$^-$ (grey bars) and CCR7$^+$ (red bars) cells (n = 4 separate cultures). (C) CD44 and CD62L expression in T cells exposed to ova-pulsed BM cell cultures sorted into CCR7$^-$ and CCR7$^+$ cells (n = 3 separate cultures). (D) Tissue location of PKH-67-labeled DC populations 48 h post-injection expressed as a percentage of all viable cells recovered from the tissues. Control = PBS only injection. Cells mock sorted, but not fractioned, remain largely at the footpad injection site, while CCR7-selected cells have largely migrated to the draining lymph node. The numbers of CCR7$^+$ cells in the non-sorted population were equivalent to those in the sorted population. (E) Analysis of DLN populations at date of cull in subcutaneous B16.ova-tumour-bearing mice treated with CCL19-reagent-exposed BMDC cultures, mock sorted or CCR7$^+$ sorted. The CCR7$^+$ sorted cells induced significantly higher percentages of SIINFEKL tetramer$^+$ CD8 T cells in the draining pLN compared to PBS controls or the CCL19-exposed but unsorted population (Ei). Both DC populations induced significantly higher numbers of memory T cells in the draining LN, but this effect reached greater signficance using CCR7$^+$ sorted cells (Figure 1Eii). n = 6 or 7 mice per group. Data are presented as mean ± SEM error bars. Statistical analysis was by one-way ANOVA (B,E), two-way ANOVA (C, D) with Bonferroni's Multiple Comparisons Test: n.s. is not significant, $^*P < 0.05$; $^{**}P < 0.01$; $^{***}P < 0.001$; $^{****}P < 0.0001$

2.6 | Statistical analyses

Data are presented as mean ± SEM. Statistical analyses were performed using GraphPad Prism 5 and 9 (GraphPad Software, La Jolla, CA, USA). Student's *t*-test 2-tailed and one and two-way ANOVA followed by Bonferroni's multiple comparisons post-test were used (details in figure legends). Tumor survival scores were assessed using Log-Rank (Mantel-Cox) test. Differences were considered statistically significant when $P < 0.05$. *P* values < 0.01 and < 0.001 are also reported where appropriate.

3 | RESULTS AND DISCUSSION

3.1 | Phenotypic characterization of CCR7-sorted DCs

BM in vitro cultures contained a majority F4/80$^-$ CD11c$^+$ zbtb46$^+$ DC population. Expression of CCR7 was most prevalent in the CD11c$^+$ zbtb46$^+$ population. CCR7$^-$ cells included CD11c$^+$zbtb46$^+$, CD11c$^+$ zbtb46$^-$, and F4/80$^+$ CD11c- cells. (Figure 1Ai). The CCR7$^+$ population thus represents a homogeneous population of DC,[20] while the

CCR7$^-$ population contains a mixture of DCs, Mϕs, and other myeloid cells. CCR7$^+$ cells were sorted from this mixed population using the bCCL19-sorting strategy[17] (Fig. 1Aii). Henceforth, we refer to 3 cellular populations: (i) mock sorted DCs; (ii) sorted DCs (cells enriched for CCR7 expression), and (iii) CCR7− cells (the cells left from the unsorted population after removal of the CCR7$^+$ cells).

Next, we examined the expression of conventional markers of DC maturity on the sorted cells. In contrast to CCR7$^-$ cells, the sorted CCR7$^+$ cells expressed markedly higher levels of MHCI, MHCII, CD40, CD86, and CD80 (Fig. 1B) indicating increased competency for Ag presentation and T cell stimulation. We used OT-I CD8$^+$ T cells to examine T-cell activating capacity of ova-pulsed CCR7$^+$ and CCR7$^-$ cells. The CCR7$^+$ cells preferentially expanded a more mature CD44$^+$CD62L$^-$ effector/memory CD8$^+$ T cell phenotype while the CCR7$^-$ supported less mature CD44$^-$CD62L$^-$ CD8$^+$ T cell populations over the course of 7 days T cell expansion in vitro (Fig. 1Ci and ii).

CCR7$^-$ cells expressed detectable levels of a number of inflammatory chemokines, while these were either not expressed, or expressed at lower levels, by the sorted CCR7$^+$ cells (Supplementary Fig. 1A). In contrast, the CCR7$^+$ DCs expressed elevated levels of chemokines binding to CCR4 (CCL17 and CCL22) and CXCR6 (CXCL16) (Supplementary Fig. 1B), which are involved in the attraction of effector/memory T cell populations, as well as regulatory T cells.[21,22] These data therefore suggest that, in contrast to their CCR7$^-$ counterparts, the CCR7$^+$- sorted cells are more primed for development of a protective adaptive immune response through the attraction of CD8$^+$ and CD4$^+$ T cells.

In keeping with roles for CCR7 in cell migration to LNs,[9] the CCR7$^+$ sorted DC population migrated very efficiently from the footpad injection site to the draining popliteal LN (pLN) (Fig. 1D). In contrast, the mock-sorted population, containing an identical number of CCR7$^+$ cells, migrated poorly (Fig. 1D). This indicates that sorting CCR7$^+$ cells to homogeneity confers a benefit, and the injection of mixed populations results in poor migration of DCs to the DLN irrespective of the presence of a substantial number of CCR7$^+$ cells.

Exposure of mixed cell populations to the bCCL19 reagent could potentiate in vivo cell migration and initiation of immune reponses. Cells were generated that had all been exposed to the bCCL19-SAPE reagent, one part was sorted into CCR7$^+$ cells, and the other mock-sorted. These cells were injected into the footpad as before (normalized to contain equal numbers of CCR7+ cells), and the mice were challenged subcutaneously 24 h later with B16-OVA tumor cells (23 and see the following section). We assayed the phenotype and Ag-specificity of T cells in the pLN draining the foot pad. The CCR7+ cell population induced significantly higher percentages of SIINFEKL tetramer+ CD8 T cells in the draining pLN compared to saline controls, whereas CCL19-exposed but unsorted population did not induce significantly more tetramer-positive cells than saline alone (Fig. 1Ei.). Both DC populations induced significantly higher numbers of memory T cells in the draining LN compared to saline alone, which may suggest a positive DC priming role for CCL19 exposure, but this effect reached greater significance using CCR7$^+$ sorted cells (Fig. 1Eii.).

Together, these data demonstrate that sorting for CCR7 enriches a population of cells with enhanced LN homing and T cell activation competence. Our data further indicate the CCR7$^-$ cells in the mixed population exert a negative effect when co-injected with equivalent numbers of CCR7$^+$ cells. The positive effect of CCL19-based cell purification cannot be replicated by simple incubation of the mixed DC population with CCL19.

3.2 | Sorted DCs display enhanced antitumor activity in vivo

We next tested the relative abilities of sorted, and mock-sorted, unfractioned, DCs to give rise to protective antitumor immune responses. As a model system, we used the subcutaneous B16.ova melanoma model[23] which expresses ovalbumin as a tumor-specific neo-Ag.

Again, the number of CCR7$^+$ cells in the unsorted population injected into recipient mice was equivalent to the number of CCR7+ -sorted DCs. In this model (Supplementary Fig. 2A) ova-peptide pulsed DCs were injected into the footpad 1 day before subcutaneous tumor injection. Tumors developed for 17 days at which time all animals were culled and tissue harvested for analysis. While the unsorted DCs did not alter tumor development, the sorted DCs had a significant effect on tumors with a 25% reduction in tumor size observable throughout the course of the experiment (Figure 2A). No differences were noted in time-to-initiation of tumor development. These data demonstrate that, in the context of an aggressively growing neoantigen-expressing tumor, sorted DCs are superior to unsorted DCs, containing a numerical equivalence of CCR7+ cells, in mediating antitumor immune responses.

As shown in Figure 2Bi, and in keeping with the enhanced LN migration of DCs from the injection site, we found higher numbers of ova-specific CD8+ T cells in the footpad-draining pLNs of mice receiving sorted DCs compared to unsorted DCs. In contrast, we saw no difference in numbers of ova-specific CD8+ T cells in the non-draining inguinal LNs (iLN) (Fig. 2Bii) thus the anti-ova response is specifically increased in the LNs draining the DC injection site. Notably, in the pLNs (Fig. 2Ci) there was a specific increase in the numbers of ova-responsive naive and central memory CD8+ T cells. In contrast, there was a reduction in central memory T cell numbers in the iLNs of mice injected with both unsorted and sorted DCs (Fig. 2Cii).

These data demonstrate that CCR7-sorted DCs have enhanced antitumor activity compared to unsorted cells associated with improved migration to draining LNs and induction of systemic central memory T cell responses.

3.3 | Double prophylactic administration of sorted DCs enhances antitumor responses

Next, we examined whether 2 DC administrations amplified the improvement seen after 1 DC injection (Supplementary Fig. 2B). These experiments were not run over a set time course, rather tumors were

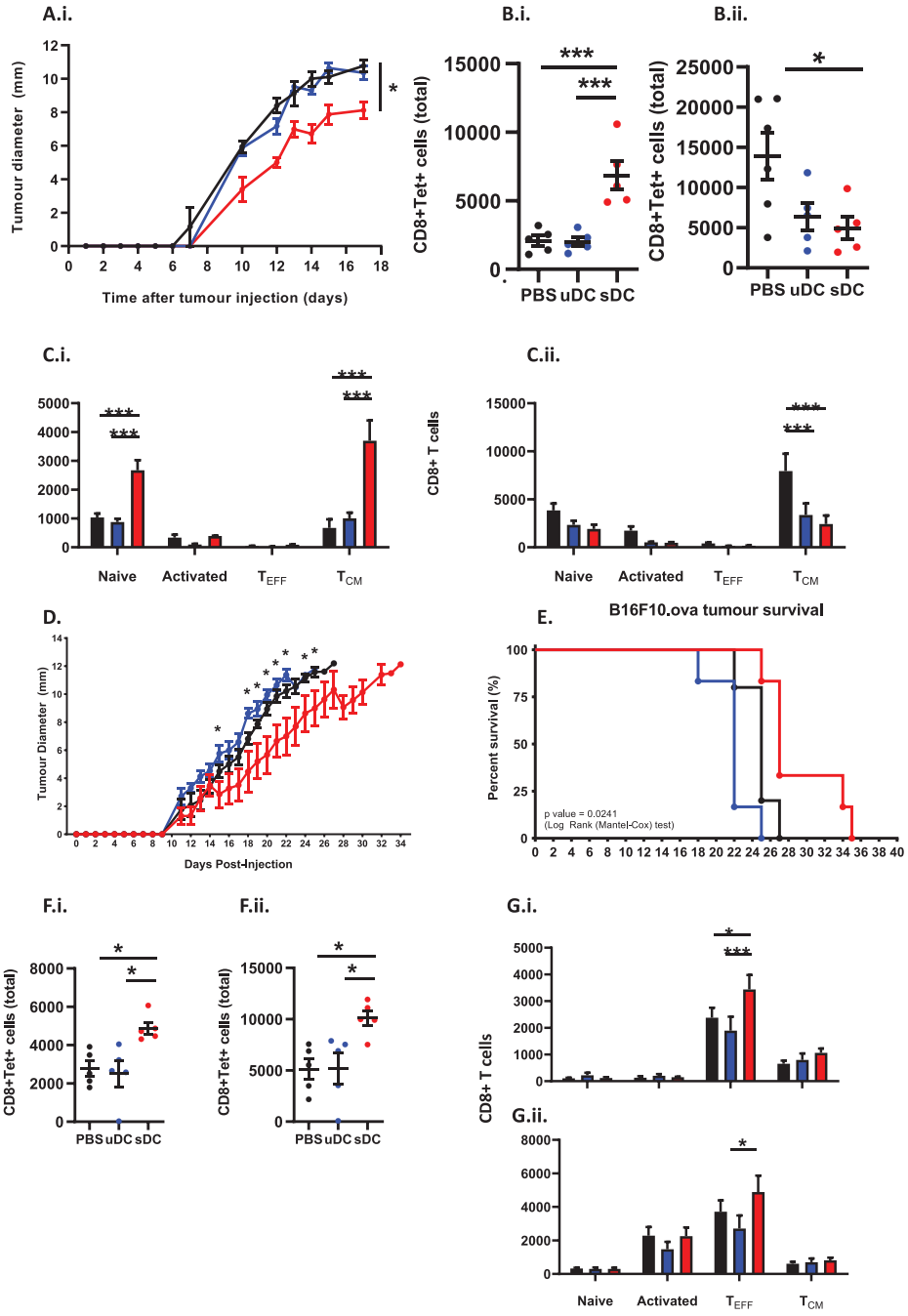

FIGURE 2 CCR7-sorted dendritic cells trigger enhanced antitumor immune responses. (A) graph of subcutaneous tumor growth over the 17 days of the single dendritic cell injection model. Black dots: PBS injected mice; blue dots: unsorted (mock sorted) BM dendritic cell (uDC) injected mice; red dots: CCR7$^+$ dendritic cell (sDC) injected mice ($n = 5$; $^*P < 0.05$ for sDC to both PBS and uDC groups). (B) Numbers of ova-tetramer + CD8 T cells in the (i) injection site draining popliteal (pLN) and (ii) tumor-draining inguinal lymph nodes (iLN). (n = 5; data points represent individuals). (C) phenotypic characterization of T cell populations in the (i) draining popliteal and (ii) non-draining iLNs. Black bars: PBS injected mice; blue bars: uDC injected mice; red bars: sDC injected mice (n = 5). (D) Graph of subcutaneous tumor growth over the 30 days of the double dendritic cell injection model ($n = 5$; $^*P < 0.05$ for sDC to both PBS and uDC groups). (E) Graph indicating mouse survival (time to cull) in a double dendritic cell injection model. Black line represents PBS injection; blue line represents uDC and red line represents sDC (n = 5). (F) Numbers of ova-tetramer + CD8 T cells in the (i) draining popliteal and (ii) non-draining iLNs. Black dots: PBS injected mice; blue dots: uDC injected mice; red dots: sDC injected mice (n = 5; data points represent individuals). (G) phenotypic characterization of T cell populations in the (i) draining popliteal and (ii) non-draining iLNs. Black bars: PBS injected mice; blue bars: unsorted dendritic cell injected mice; red bars: CCR7$^+$ dendritic cell injected mice (n = 5). Data are presented as mean ± SEM error bars. Statistical analysis was by one-way ANOVA (A, B, D, F) or two-way ANOVA (C, G) with Bonferroni's Multiple Comparisons Test, and tumor survival score (E) was assessed using Log-Rank (Mantel Cox) test. $^*P < 0.05$; $^{***}P < 0.0001$

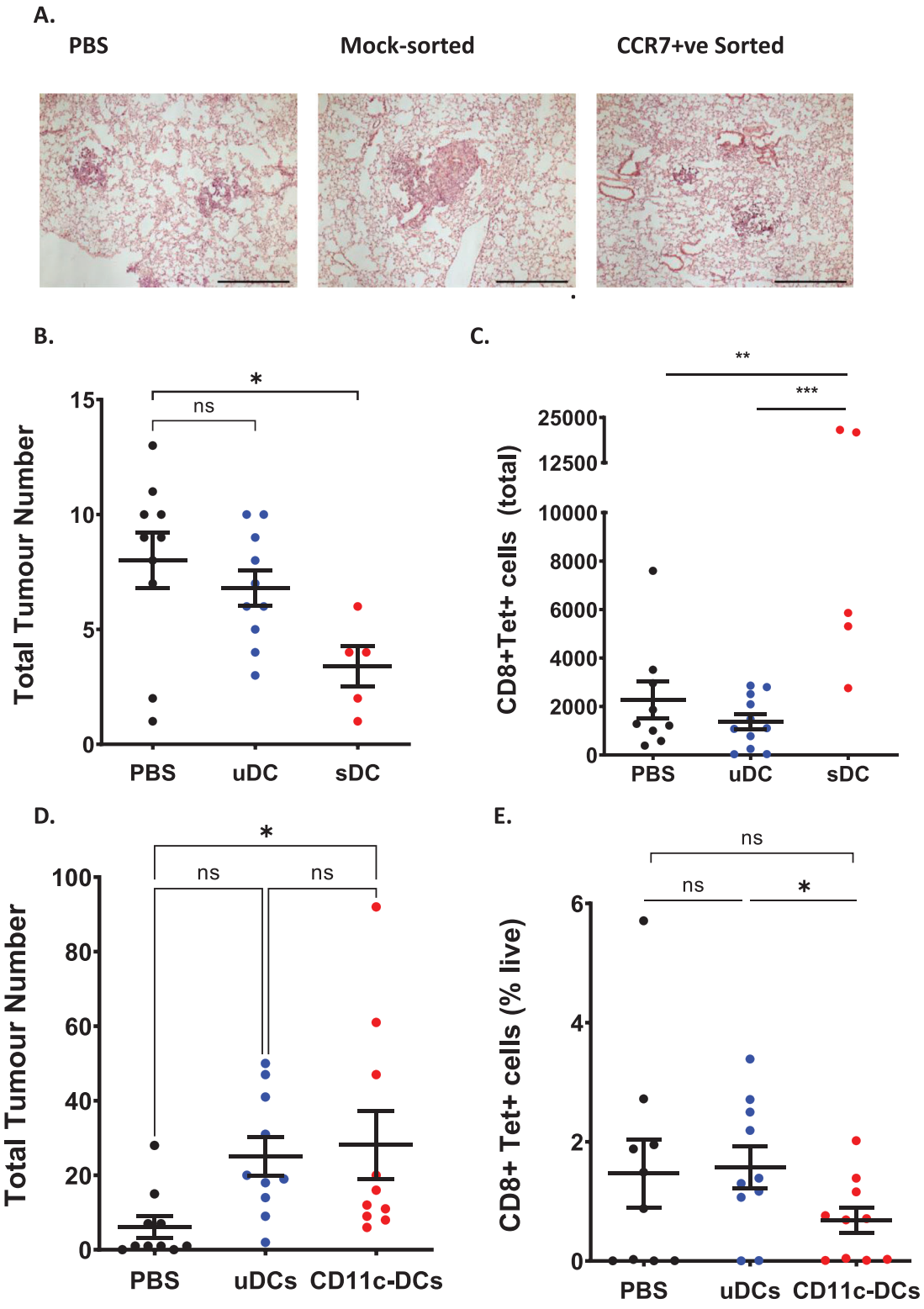

FIGURE 3 CCR7-sorted dendritic cells also enhance immune responses against metastatic tumours. (A) Exemplar histological analyses of pulmonary metastatic deposits from PBS injected, Unsorted (mock-sorted) cell injected, and CCR7^{+} cell injected mice. (B) Numbers of metastatic lesions in the lungs of mice as assessed in histological cross-sections of tumor-bearing lungs (n = 10 for PBS and uDC; n = 5 for sDC). (C) Ova-tetramer positive CD8+ T cell numbers in the popliteal lymph nodes draining the dendritic cell injection site (n = 10 for PBS and uDC; n = 5 for sDC). (D and E). Comparison of Mock sorted (uDC) and CD11c-sorted (CD11c-DC) cells in lung metastasis model. When mice were culled at the end of the experiment (day 14) there was no reduction in the numbers of tumors detected (CD11c group has significantly more) (D) and no increases in Ova-specific T cells in the draining lymph node (E). Data are presented as individual data points with mean ± SEM error bars. Statistical analysis was by one-way ANOVA. *$P < 0.05$; **$P < 0.01$; ***$P < 0.0001$

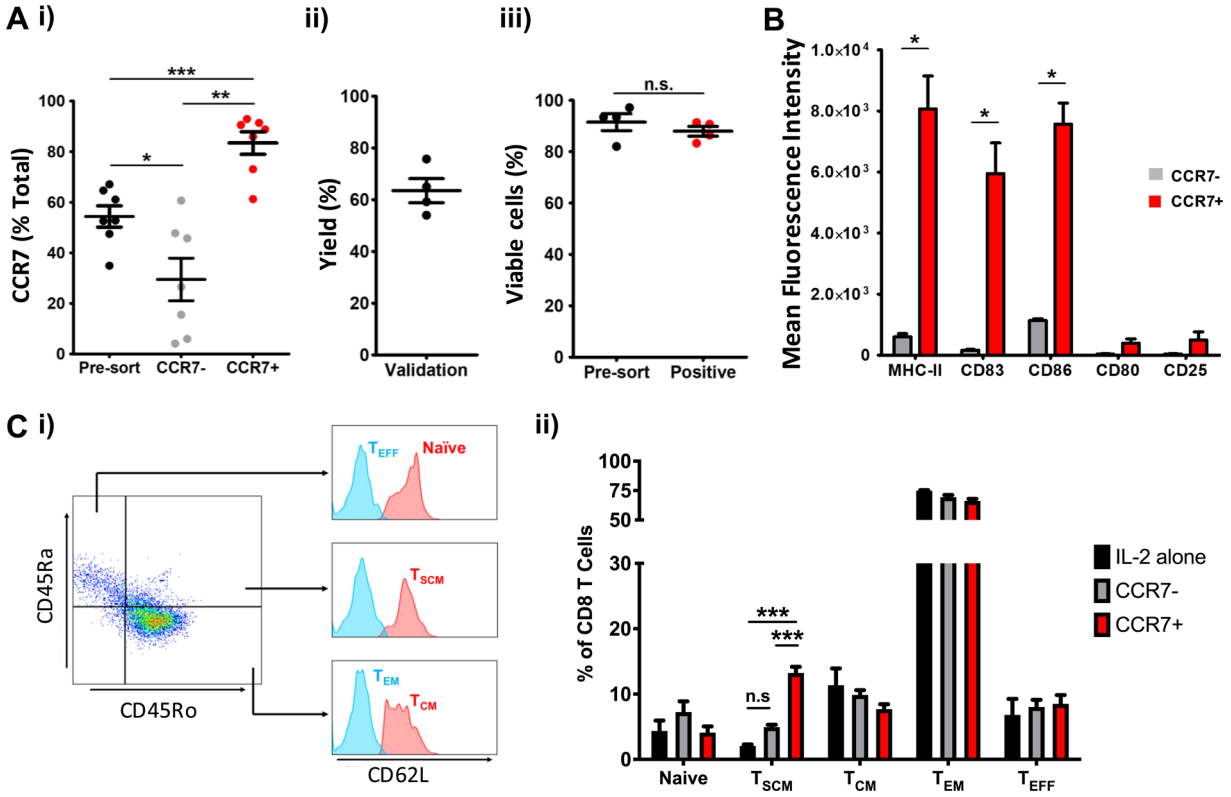

FIGURE 4 Adapting the chemokine sorting protocol for clinical-grade use. (A) (i) Chemokine-based sorting enriches moDCs from being approximately 55% CCR7$^+$ to in excess of 80% CCR7$^+$ (n = 7). (ii) Yields of approximately 60% are routinely obtained following sorting (n = 4). (iii) Sorted cells are approximately 90% viable (n = 4; data points represent individuals). (B) Expression of markers of Ag-presenting competence in CCR7$^-$ (grey bars) and CCR7$^+$ (red bars) moDCs (n = 5). (C) (i) Gating strategy showing flow cytometry gates for naïve, effector (T_{EFF}), stem cell memory (T_{SCM}), and central memory (T_{CM}) T cells. (ii) Quantification of the different T cell populations showing a specific increase in T_{SCM} cells in response to CCR7 + moDC. Data are presented as mean ± SEM error bars. Statistical analysis was by one-way ANOVA (Ai) or by two-tailed Students *t*-test (Aii, Aiii, Cii). n.s. is not significant. $^*P < 0.05$; $^{**}P < 0.01$; $^{***}P < 0.0001$

allowed to develop to a diameter necessitating animal cull allowing for a comparison of the relative "survival" of mice receiving the sorted or unsorted DCs. We observed a 40–50% reduction in tumor growth, as measured by tumor-diameter, in mice receiving the double prophylactic administration of sorted CCR7$^+$ DC, compared to unsorted DCs or PBS control (Fig. 2D). This was associated with significantly increased overall survival of mice receiving sorted DCs compared to mice receiving either unsorted DCs or PBS control ($P = 0.0241$). Analysis of ova-specifc CD8$^+$ T cells indicated elevated numbers in the footpad-draining pLNs (Fig. 2Fi) but increased numbers were also seen in the iLN (Fig. 2Fii). Analysis of the specific CD8$^+$ T cell phenotypes in these tissues (Fig. 2Gi and Gii) revealed that they were predominantly of an effector phenotype.

Thus double administration of sorted DCs leads to a sustained increase in tumor Ag-specific T cells over a single injection. This amplified T cell response is associated with a reduction in tumor development and increased "survival." The Ag-specific T cell phenotype is now skewed in favor of an effector phenotype suggesting that repeated doses of CCR7$^+$ DCs lead to the production of a greater number of effector T cells.

3.4 | Sorted DCs display enhanced Ag-specific T cell reponses in a model of pulmonary metastasis

The B16 model also lends itself to the development of pulmonary metastases (Supplementary Fig. 2C) following intravenous injection.[24] As shown (Fig. 3A), the metastatic deposits that developed in mice receiving either PBS control or mock sorted, unfractionated cells or CCR7$^+$ cells were histologically indistinguishable. However, mice receiving CCR7$^+$ DCs, in contrast to the unsorted cells, developed significantly fewer metastatic deposits in the lung. Indeed, we observed a 50% reduction in metastasis number in mice receiving sorted DCs compared to unsorted cells or PBS administration. This was associated with increased numbers of ova-specific CD8$^+$ T cells in the pLN (Fig. 3C). These data demonstrate that the CCR7$^+$, compared to unsorted, DCs can induce an effective immune response against disseminated, metastatic cancers that leads to reduced metastatic deposits.

In further investigations using this model, cells sorted based on expression of CD11c were compared to mock-sorted DC. When mice were culled at the end of the experiment (day 14) there were no

differences in the numbers of lung tumors or ova-specific T cells in the draining lymph node. Thus treatment with this differently sorted population of mature DCs that contains a mixture of CCR7$^+$ and CCR7$^-$ cells does not lead to a reduction in tumor number in this model (Fig. 3D).

3.5 | This approach is translatable to human therapies

The use of cells in human therapy requires their production under the most stringent GMP conditions. We generated human DCs from CD14-purified cells in Xeno-free medium[26] the most commonly used in vitro source of therapeutic DCs. As our CCL19 reagent is chemically synthesized, it can also be produced to the appropriate GMP reagent grade (Almac Sciences). We sorted human DCs using the TYTO clinical-grade cell sorter (www.miltenyibiotec.com/upload/assets/IM0020121.PDF). Using this clinical-grade disposable cartridge sorter, we were able to sort, with high efficiency and yield, large numbers of CCR7$^+$ DCs from a mixed population of human moDCs (Fig. 4Ai and Aii). This differs from mouse cultures as all cells in the human cultures are DCs (Supplementary Fig. 3), sorting aims to isolate the migration-competent cells. These CCR7$^+$ sorted cells are viable (Fig. 4Aiii) and, as with their mouse counterparts, express very high levels of molecules involved in Ag presentation and stimulation of T cells (Fig. 4B). We next tested their ability to activate human T cells by incubating CCR7$^+$ and CCR7$^-$ DCs with autologous T cells and EBV Ag for 10 days in vitro and then assessing T cell phenotypes using flow cytometry. The CCR7$^+$ sorted DCs were capable of significantly enhancing the persistence of stem cell memory CD8$^+$ T cells in vitro while the CCR7$^-$ DC were not (Fig. 4C). Overall these data demonstrate that the experimental approach developed for sorting mouse cells using CCL19 is feasible for human DC and is of potential direct clinical applicability using identical reagents.

We have therefore shown that CCR7$^+$-selected DCs have enhanced LN homing, Ag presentation, and T cell stimulation capacity that correlate with increased protection in both the subcutaneous B16 melanoma model and the intravenous model of pulmonary metastasis. Importantly, our data show the CCR7$^+$ sorted cells are highly enriched for expression of Zbtb46 and demonstrate superior function to a population of unselected cells containing the same number of CCR7$^+$ cells. We have shown that separating the CCR7$^+$ cells from the non-CCR7 expressing cells is required for the improved function of the CCR7$^+$ cells – this emphasizes the value of the sorting procedure described for therapeutic DC therapy. Future studies should concentrate on using CCR7$^+$ DC to treat established tumors, for example, following resection or chemotherapy. In vitro data show CCR7$^+$ DCs, compared to CCR7$^-$ cells, can uniquely prime Ag-specific naïve and memory T cells, both of which contribute to an antitumor response and are therefore highly desirable in a therapeutic context.[25] In addition, we demonstrate enhanced expression of T cell chemoattractants by sorted DCs suggesting that they may be better equipped to mediate interactions with T cells upon arrival in the LN.

ACKNOWLEDGMENTS

G.J.G. is supported by a Programme Grant from the Medical Research Council and a Wellcome Trust Senior Investigator Award. G.J.G. also receives support from a Wolfson Royal Society Research Merit Award. P.B. was supported by an NHS National Services Scotland Postgraduate studentship awarded to J.D.M.C. and G.J.G.

AUTHORSHIP

P.B. was associated with Investigation, data curation and formal analysis, wrote the original draft, and reviewed, edited, and revised the final manuscript. A.J.H., R.S.C., M.L.L.B., and C.A.A.H. were associated with investigation, data curation and formal analysis, and reviewed, edited, and revised the final manuscript. J.D.M.C. and G.J.G. were associated with conceptualization, data curation and formal analysis, and reviewed, edited, and revised the final manuscript.

DISCLOSURE

The authors declare that they have no conflict of interest.

ORCID

Paul Burgoyne https://orcid.org/0000-0003-4285-3266
Alan J Hayes https://orcid.org/0000-0003-2708-6230
John DM Campbell https://orcid.org/0000-0001-7752-7642
Gerard J Graham https://orcid.org/0000-0002-7801-204X

REFERENCES

1. Miliotou AN, Papadopoulou LC. CAR T-cell therapy: a new era in cancer immunotherapy. *Curr Pharm Biotechnol*. 2018;19:5-18.
2. Bianco P. Mesenchymal" stem cells. *Annual Review of Cell and Developmental Biology*. 2014;30:677-704.
3. van Willigen WW, Bloemendal M, Gerritsen WR, Schreibelt G, de Vries IJM, Bol KF. Dendritic cell cancer therapy: vaccinating the right patient at the right time. *Frontiers in Immunology*. 2018;9.
4. Aarntzen E, Srinivas M, Schreibelt G, Heerschap A, Punt CJA, Figdor CG, et al. Reducing cell number improves the homing of dendritic cells to lymph nodes upon intradermal vaccination. *Oncoimmunology*. 2013;2.
5. de Vries IJM, Krooshoop D, Scharenborg NM, Lesterhuis WJ, Diepstra JHS, van Muijen GNP, et al. Effective migration of antigen-pulsed dendritic cells to lymph nodes in melanoma patients is determined by their maturation state. *Cancer Research*. 2003;63:12-7.
6. Lesterhuis WJ, de Vries IJM, Schreibelt G, Lambeck AJA, Aarntzen E, Jacobs JFM, et al. Route of administration modulates the induction of dendritic cell vaccine-induced antigen-specific t cells in advanced melanoma patients. *Clinical Cancer Research*. 2011;17:5725-35.
7. Griffith JW, Sokol CL, Luster AD. Chemokines and chemokine receptors: positioning cells for host defense and immunity. *Annu Rev Immunol*. 2014;32:659-702.
8. Bachelerie F, Ben-Baruch A, Burkhardt AM, Combadiere C, Farber JM, Graham GJ, et al. International union of pharmacology. LXXXIX. update on the extended family of chemokine receptors and introducing a new nomenclature for atypical chemokine receptors. *Pharmacological Reviews*. 2014;66:1-79.
9. Forster R, Davalos-Misslitz AC, Rot A. CCR7 and its ligands: balancing immunity and tolerance. *Nat Rev Immunol*. 2008;8:362-71.
10. Forster R, Schubel A, Breitfeld D, Kremmer E, Renner-Muller I, Wolf E, et al. CCR7 coordinates the primary immune response by establishing functional microenvironments in secondary lymphoid organs. *Cell*. 1999;99:23-33.

11. Okada N, Mori N, Koretomo R, Okada Y, Nakayama T, Yoshie O, et al. Augmentation of the migratory ability of DC-based vaccine into regional lymph nodes by efficient CCR7 gene transduction. *Gene therapy*. 2005;12:129-39.
12. Gonzalez FE, Ortiz C, Reyes M, Dutzan N, Patel V, Pereda C, et al. Melanoma cell lysate induces CCR7 expression and in vivo migration to draining lymph nodes of therapeutic human dendritic cells. *Immunology*. 2014;142:396-405.
13. Roberts EW, Broz ML, Binnewies M, Headley MB, Nelson AE, Wolf DM, et al. Critical role for CD103(+)/CD141(+) dendritic cells bearing CCR7 for tumor antigen trafficking and priming of T cell immunity in melanoma. *Cancer Cell*. 2016;30:324-36.
14. Lesterhuis WJ, de Vries IJM, Schreibelt G, Lambeck AJA, Aarntzen EHJG, Jacobs JFM, et al. Route of administration modulates the induction of dendritic cell vaccine-induced antigen-specific T cells in advanced melanoma patients. *Clinical Cancer Research*. 2011;17:5725-35.
15. Somanchi SS, Somanchi A, Cooper LJN, Lee DA. Engineering lymph node homing of ex vivo-expanded human natural killer cells via trogocytosis of the chemokine receptor CCR7. *Blood*. 2012;119:5164-72.
16. Jin H, Qian Y, Dai Y, Qiao S, Huang C, Lu L, et al. Magnetic enrichment of dendritic cell vaccine in lymph node with fluorescent-magnetic nanoparticles enhanced cancer immunotherapy. *Theranostics*. 2016;6:2000-14.
17. Le Brocq ML, Fraser AR, Cotton G, Woznica K, McCulloch CV, Hewit KD, et al. Chemokines as novel and versatile reagents for flow cytometry and cell sorting. *Journal of Immunology*. 2014;192:6120-30.
18. Anselmo A, Mazzon C, Borroni EM, Bonecchi R, Graham GJ, Locati M. Flow cytometry applications for the analysis of chemokine receptor expression and function. *Cytometry Part A*. 2014;85:292-301.
19. Hayes AJ, Rane S, Scales HE, Meehan GR, Benson RA, Maroof A, et al. Spatiotemporal modeling of the key migratory events during the initiation of adaptive immunity. *Frontiers in Immunology*. 2019;10.
20. Satpathy AT, KC W, Albring JC, et al. Zbtb46 expression distinguishes classical dendritic cells and their committed progenitors from other immune lineages. *J Exp Med*. 2012;209:1135-52.
21. Yoshie O, Matsushima K. CCR4 and its ligands: from bench to bedside. *International Immunology*. 2014;27:11-20.
22. Latta M, Mohan K, Issekutz TB. CXCR6 is expressed on T cells in both T helper type 1 (Th1) inflammation and allergen-induced Th2 lung inflammation but is only a weak mediator of chemotaxis. *Immunology*. 2007;121:555-64.
23. Overwijk WW, Restifo NP. B16 as a mouse model for human melanoma. *Current protocols in immunology*. 2001;20. Chapter. Unit-20.1.
24. Hansell CAH, Fraser AR, Hayes AJ, Pingen M, Burt CL, Lee KM, et al. The atypical chemokine receptor ackr2 constrains nk cell migratory activity and promotes metastasis. *The Journal of Immunology*. 2018:ji1800131.
25. Klebanoff CA, Gattinoni L, Restifo NP. Sorting through subsets: which T-cell populations mediate highly effective adoptive immunotherapy?. *Journal of immunotherapy (Hagerstown, Md: 1997)*. 2012;35:651-60.
26. Campbell JDM, Piechaczek C, Winkels G, et al. Isolation and generation of clinical-grade dendritic cells using the CliniMACS system. *Methods Mol Med*. 2005;109:55-70.

SUPPORTING INFORMATION

Additional supporting information may be found in the online version of the article at the publisher's website.

How to cite this article: Burgoyne P, Hayes AJ, Cooper RS, et al. CCR7+ dendritic cells sorted by binding of CCL19 show enhanced Ag-presenting capacity and antitumor potency. *J Leukoc Biol*. 2022;111:1243–1251.
https://doi.org/10.1002/JLB.5AB0720-446RR